Cerebral Cortex, February 2019;29: 561–572

doi: 10.1093/cercor/bhx338
Advance Access Publication Date: 5 January 2018
Original Article

ORIGINAL ARTICLE

Treatment With the Neutralizing Antibody Against Repulsive Guidance Molecule-a Promotes Recovery From Impaired Manual Dexterity in a Primate Model of Spinal Cord Injury

Hiroshi Nakagawa[1,2,5], Taihei Ninomiya[1,3,4], Toshihide Yamashita[2] and Masahiko Takada[1]

[1]Systems Neuroscience Section, Primate Research Institute, Kyoto University, Inuyama, 484-8506, Japan, [2]Department of Molecular Neuroscience, Graduate School of Medicine, Osaka University, Suita 565-0871, Japan, [3]Division of Behavioral Development, Department of System Neuroscience, National Institute for Physiological Sciences, Okazaki 444-8585, Japan, [4]Department of Physiological Sciences, School of Life Science, SOKENDAI (The Graduate University for Advanced Studies), Hayama 240-0193, Japan and [5]Present address: Sobell Department of Motor Neuroscience and Movement Disorders, Institute of Neurology, University College London, London WN1C 3BG, UK

Address correspondence to Hiroshi Nakagawa, Sobell Department of Motor Neuroscience and Movement Disorders, Institute of Neurology, University College London, Queen Square, London WN1C 3BG, UK. Email: h.nakagawa@ucl.ac.uk

Abstract

Axons in the mature mammalian central nervous system have only a limited capacity to grow/regenerate after injury, and spontaneous recovery of motor functions is therefore not greatly expected in spinal cord injury (SCI). To promote functional recovery after SCI, it is critical that corticospinal tract (CST) fibers reconnect properly with target spinal neurons through enhanced axonal growth/regeneration. Here, we applied antibody treatment against repulsive guidance molecule-a (RGMa) to a monkey model of SCI. We found that inhibition of upregulated RGMa around the lesioned site in the cervical cord resulted in recovery from impaired manual dexterity by accentuated penetration of CST fibers into laminae VII and IX, where spinal interneurons and motoneurons are located, respectively. Furthermore, pharmacological inactivation following intracortical microstimulation revealed that the contralesional, but not the ipsilesional, primary motor cortex was crucially involved in functional recovery at a late stage in our SCI model. The present data indicate that treatment with the neutralizing antibody against RGMa after SCI is a potential target for achieving restored manual dexterity in primates.

Key words: corticospinal tract, manual dexterity, primates, repulsive guidance molecule-a, spinal cord injury

Introduction

Manual dexterity as represented by precision grip is a skilled motor behavior characteristic of higher primates. It is generally accepted that manual dexterity is closely related to direct connectivity of the corticospinal tract (CST), arising from the motor cortex (MI) to the motoneurons of the cervical cord that control the distal hand muscles (Lemon 1993). A spinal cord injury (SCI) disrupts the CST and often causes permanent

disability with sensorimotor dysfunction. Therefore, the CST has become an essential target for SCI treatment (GrandPré et al. 2002; Oudega and Perez 2012). However, the mature mammalian central nervous system (CNS) has only a limited capacity to grow/regenerate once injured because of a number of inhibitory factors, including those that relate to axon guidance molecules (Yiu and He 2006).

Repulsive guidance molecule-a (RGMa) is one such axon guidance molecule. Originally identified in the visual system (Stahl et al. 1990; Monnier et al. 2002), RGMa has now been implicated in neuronal survival, proliferation, and differentiation (Matsunaga et al. 2004, 2006; Lah and Key 2012). RGMa was upregulated around the lesioned site after SCI in rodents (Schwab et al. 2005), and treatment with the neutralizing antibody against RGMa has been shown to accelerate axonal regrowth and sprouting from the CST following thoracic cord lesions (Hata et al. 2006). On the other hand, to promote functional recovery via enhanced sprouting of CST fibers after CNS injuries, such fibers are required to extend toward an appropriate locus and reconnect with target spinal neurons (Wahl et al. 2014). It has recently been reported in macaque monkeys that a number of CST fibers derived from the contralesional primary MI after SCI sprout below the lesioned site into laminae VII and IX, where spinal interneurons and motoneurons are located, respectively (Nakagawa et al. 2015). Moreover, the relative number of sprouting fibers significantly increased in lamina IX (Nakagawa et al. 2015). By contrast, the sprouting CST fibers chiefly terminate within the medial gray matter in rodents (Hata et al. 2006; Vavrek et al. 2006). These results suggest that the mechanisms underlying axonal remodeling that leads to the recovery of motor functions after SCI may differ in higher primates and rodents. Therefore, it is important to understand axonal remodeling specific to higher primates for restoration of manual dexterity after SCI. Concerning application to human patients with SCI, it is also crucial to confirm whether RGMa suppression promotes recovery from impaired manual dexterity.

The present study aimed at establishing an antibody treatment against RGMa in higher primates. Our results indicate that treatment with the neutralizing antibody against RGMa is critical to achieve restored manual dexterity after SCI.

Materials and Methods

Animals

Twelve rhesus monkeys (*Macaca mulatta*, aged 3–5 years, 3.8–5.4 kg) of either sex were used in the present study: 3 lesioned monkeys for treatment with a control antibody (Ctrl-A to Ctrl-C), 4 lesioned monkeys for treatment with the anti-RGMa antibody (RGMa-A to RGMa-D), and 5 normal monkeys for molecular biological (western blotting) and histological (histochemical, immunohistochemical, and in situ hybridization) analyses. The experimental protocols were approved by the Animal Welfare and Animal Care Committee of the Primate Research Institute, Kyoto University. All experiments were conducted in accordance with the Guidelines for the Care and Use of Laboratory Primates (Ver. 3, 2010) set by the Primate Research Institute of Kyoto University, Japan.

Anti-RGMa Antibody

We used an anti-human RGMa antibody (mouse IgG; IBL) as a neutralizing antibody against RGMa in the present study. The antibody was raised against the C-terminal sequence of human RGMa, LYERTRDLPGRAAAGL. The protein sequence of human RGMa fully corresponds with that for macaque monkeys. It has previously been reported that the antibody has an inhibitory effect on human RGMa obtained from peripheral blood mononuclear cells of human patients with multiple sclerosis (Muramatsu et al. 2011).

Western Blotting

Following sedation with ketamine hydrochloride (10 mg/kg, i.m.) and xylazine hydrochloride (1 mg/kg, i.m.), an intact monkey was anesthetized deeply with sodium pentobarbital (50 mg/kg, i.v.) and perfused transcardially with 0.1 M phosphate-buffered saline (PBS; pH 7.4). The MI (digit region) and the spinal cord (C7–Th1 segments) were harvested and homogenized in a lysis buffer, comprising 50 mM Tris-HCl (pH 7.8) with 150 mM NaCl, 1 mM EDTA, 2 mM Na_3VO_4, 1% NP-40, and protease inhibitor cocktail. After centrifugation at 13 000 × *g* for 20 min at 4 °C, samples were lysed using equal amounts of 2× sample buffer, comprising 250 mM Tris-HCl, 4% sodium dodecyl sulfate, 20% glycerol, 0.02% bromophenol blue, and 5% β-mercaptoethanol, and then proteins were boiled for 5 min at 95 °C. The mixed proteins were separated on sodium dodecyl sulfate polyacrylamide gel electrophoresis and transferred to a polyvinylidence fluoride membrane (Millipore). The membrane was blocked with 5% skim milk in 0.01 M PBS containing 0.05% Tween-20 and then incubated with anti-RGMa antibody (IBL). After several washes, the membrane was incubated with horseradish peroxidase-linked anti-mouse IgG antibody (1:5000; Cell Signaling Technology). The detection was carried out with an ECL chemiluminescence system (GE Healthcare). As control samples, human- and mouse-recombinant RGMa proteins (R & D systems) were used.

Experimental Time-Course

The experimental time-course is summarized in Figure 1N. The monkeys were trained with 2 behavioral tasks, a reaching/grasping task and a modified Brinkman board test for 2–3 months prior to SCI. To reduce the interanimal variability in the modified Brinkman board test (Freund et al. 2006, 2009), pairs of monkeys who exhibited similar baselines before SCI (i.e., Ctrl-A and RGMa-A, Ctrl-B and RGMa-B, and Ctrol-C and RGMa-C) usually underwent simultaneous behavioral analyses. After SCI, the 2 behavioral tasks were performed to assess the extent of recovered forelimb movements over 14 weeks. Following all behavioral analyses, the digit regions of the contralesional and ipsilesional MI were identified in the anti-RGMa antibody-treated monkeys using intracortical microstimulation (ICMS), and then muscimol was injected into the identified digit regions to inactivate neuronal activity therein. To examine sprouting CST fibers below the lesioned site, biotinylated dextran amine (BDA) was injected into the contralesional MI 7 weeks prior to sacrifice. To label spinal motoneurons through the median nerve on the SCI side, wheat germ agglutinin-conjugated horseradish peroxidase (WGA-HRP) was infused from the cut end of the nerve 4 days prior to sacrifice. One of the 4 monkeys (RGMa-B) who were treated with the anti-RGMa antibody was excluded from the electrophysiological/pharmacological and histological analyses, because this monkey died of an unknown cause shortly after behavioral analyses.

Behavioral Analyses

We investigated whether treatment with the neutralizing antibody against RGMa might promote recovery from impaired manual dexterity after SCI. To assess the extent to which the skilled motor behavior was restored in our SCI model, the 2 behavioral tasks were performed. In the tasks, monkeys were trained to take out pellets from vertical and horizontal slots. Each

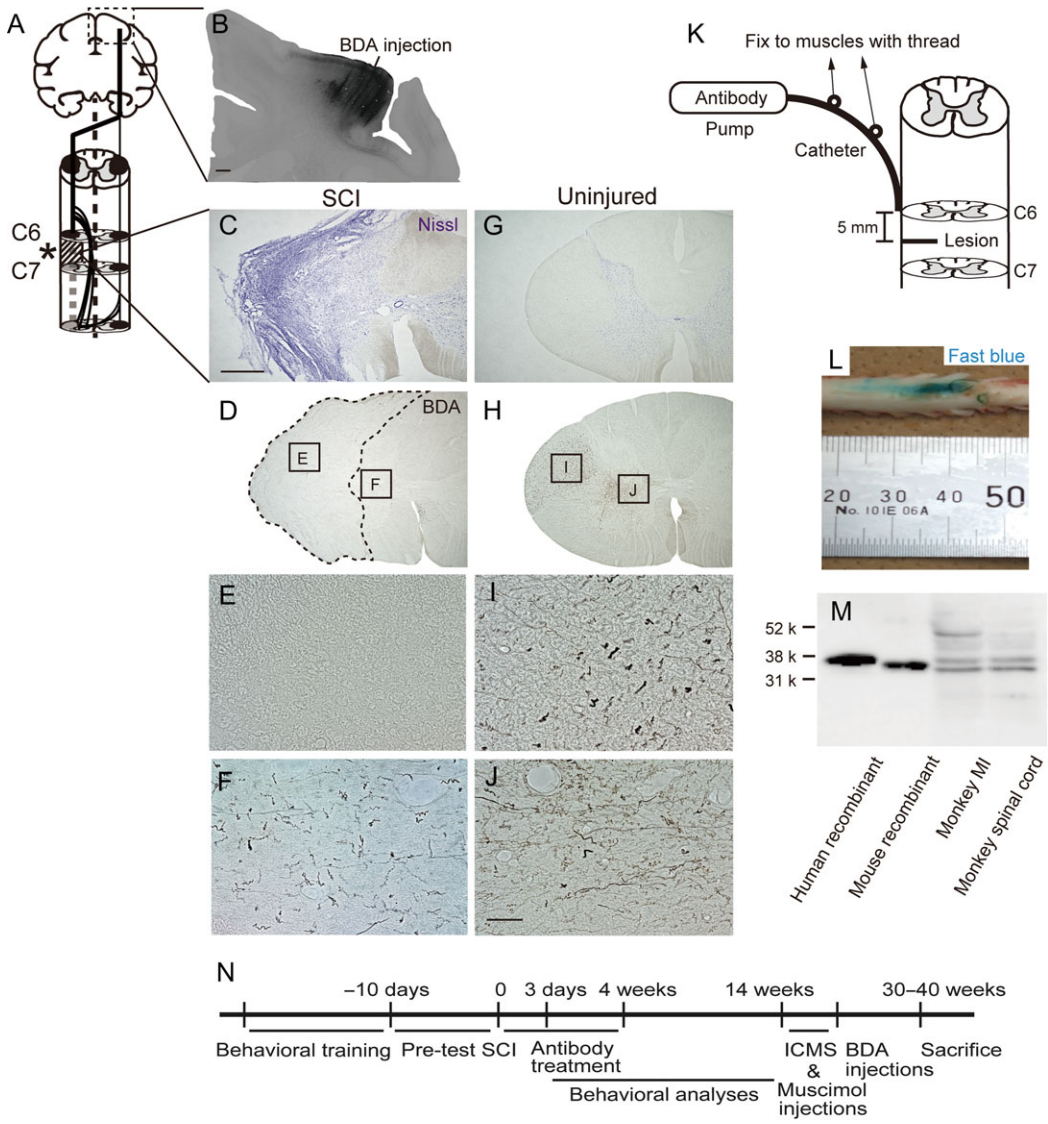

Figure 1. SCI model and experimental time-course. (*A*) Schematic diagram showing our primate model of SCI. Unilateral lesions were made at the border of segments C6 and C7. The asterisk indicates the lesioned site. (*B*) Example of the injection site in the contralesional MI. (*C* and *G*) Nissl-stained transverse sections in the injured (SCI) and uninjured spinal cords. The strongly stained area represents the lesion extent in panel *C*. (*D* and *H*) Transverse sections labeled with BDA injected into the contralesional or contralateral MI in the injured or uninjured spinal cord, respectively. The dotted line demarcates the lesioned area in panel *D*. (*E* and *I*) Higher power magnifications of areas in the dorsolateral funiculus in panels *D* and *H*, respectively. (*F* and *J*) Higher power magnifications of areas in the medial gray matter in panels *D* and *H*, respectively. Note that BDA-labeled CST fibers extend beyond the lesioned site through the intact medial gray matter in the injured spinal cord. (*K*) Schematic diagram showing the antibody delivery system using an osmotic pump. (*L*) Anti-RGMa antibody delivered around the lesioned site via an osmotic pump. To visualize the extent of antibody infusion, Fast blue was used. (*M*) Western blot analysis of the anti-RGMa antibody. The antibody crosses to the MI and the spinal cord of a rhesus monkey. (*N*) Experimental time-course. Scale bars, *B* and *C*: 1 mm for *B*–*D* and *G*, *H*, for *B*, *C*, *E*; *J*: 50 μm for *E*, *F*, *I*, and *J*.

behavioral analysis was carried out on the 3rd, 5th, 7th, and 10th day after SCI, and then twice a week until the 14th week.

Reaching/grasping Task

This task was performed to assess quantitatively the extent of recovery of dexterous manual movements as previously described (Nakagawa et al. 2015). Briefly, the monkeys were seated in a primate chair, and an acrylic board which consisted of 3 vertical or horizontal slots was placed in front of the chair (Fig. 4A,B). Each slot was filled with a small pellet (diameter, 9 mm). The monkeys reached for the vertical or horizontal slots and attempted to pick up 3 pellets within 10 s in each trial. We analyzed how many pellets the monkeys successfully collected in each session (7 trials). Data were expressed as the ratio of the number of collected pellets to the total number per session (21 pellets; 3 pellets × 7 trials) in each of the vertical-slot and horizontal-slot tasks.

Modified Brinkman Board Test

The Brinkman board test was originally created to assess manual dexterity after SCI at the cervical cord level in macaque monkeys (Rouiller et al. 1998). Later, Freund et al. (2006, 2009) made a minor modification for analyzing the extent of functional recovery from SCI, and named it "a modified Brinkman board test." In the present study, we applied this modified version. The monkeys were seated in a primate chair, and the Brinkman board was placed on the chair. The Brinkman board

(10 cm × 20 cm) was made of an acrylic board where a total of 50 slots (15 mm long × 8 mm wide × 6 mm deep), consisting of 25 vertical and 25 horizontal slots, were randomly located on the board (Fig. 4E). Each slot was filled with a food pellet (94 mg, banana or very berry flavor; Bioserve). In our modified Brinkman board test, each session consisted of 50 trials (25 trials for each of the vertical- and horizontal-slot tasks) and a total of 50 pellets. A trial was considered successful when the monkey grasped a pellet and conveyed it to the mouth within 30 s. A trial was considered unsuccessful when the monkey failed to grasp a pellet or dropped it on the way to the mouth. The baseline value prior to SCI was represented as the mean number of successful trials (maximum = 25) per session in each of the vertical- and horizontal-slot tasks that were performed 7 times (5 sessions per day). In each monkey, the analyzed data were evaluated as the number of successful trials per session in a daily test.

Surgical Procedures for SCI

Surgical procedures for SCI were performed as previously described with minor modifications (Nakagawa et al. 2015). Briefly, the monkeys were sedated with a combination of ketamine hydrochloride (10 mg/kg, i.m.), xylazine hydrochloride (1 mg/kg, i.m.), and atropine (0.05 mg/kg, i.m.), and then anesthetized with sodium pentobarbital (25 mg/kg, i.v.). The monkeys who were monitored with percutaneous oxygen saturation, respiration rate, heart rate, blood pressure, body temperature, and electrocardiogram were stabilized in a stereotaxic frame. The skin and axial muscles were dissected at the level of the C2–T1 segments under aseptic conditions. Subsequently, laminectomy of the C3–C7 segments was performed, and the dura mater was cut unilaterally. After identification of the dorsal roots at the C6 and C7 levels, a border between the C6 and the C7 segment was lesioned with a surgical blade (No. 11) and a special needle (27 G). The anti-RGMa antibody or control antibody (IgG from mouse serum; Sigma-Aldrich) was continuously delivered, via an osmotic pump (2ML4, Alzet) installed under the skin of the back, to the periphery of the lesioned site over 4 weeks immediately after SCI. Both the anti-RGMa and the control antibodies purified as IgGs were concentrated to 50 μg/kg/day in PBS. To estimate the extent of antibody infusion in the spinal cord, a 1% solution of Fast blue (Polysciences) was used instead of the antibody. To fix a catheter (11 cm long) attached to the osmotic pump, the top of the catheter was placed 5 mm above the lesioned site under the dura mater (intrathecal administration) following SCI, and the catheter was connected to the dura mater and surrounding muscles with a surgical suture to maintain its position during delivery of the antibody (Fig. 1K). Subsequently, spongel (Astellas) was applied on the dura mater for hemostasis, and the muscles and skin were sutured. Following the surgery, the monkeys were given an analgesic (Lepetan; Otsuka; i.m.; Indomethacin; Isei; oral, 1 week) and an antibiotic (Viccillin; Meiji Seika; i.m., 3–4 days). Four weeks later, the osmotic pump was removed from the back under general anesthesia (see above) and checked to ensure that the antibody was delivered in its entirety.

Intracortical Microstimulation

Under general anesthesia with sodium pentobarbital (25 mg/kg, i.v.), 2 pipes made of polyether ether ketone were mounted in parallel over the frontal and occipital lobes for head fixation. After partial removal of the skull over the central sulcus under aseptic conditions, 2 rectangular plastic chambers (for the contralesional MI, 37 mm long × 42 mm wide × 15 mm deep; for the ipsilesional MI, 28 mm long × 32 mm wide × 20 mm deep) were attached to the exposed skull. Several days later, each monkey was seated in a primate chair with the head fixed in a stereotaxic frame attached to the chair. A glass-coated tungsten microelectrode (0.5–1.5 MΩ at 1 kHz; Alpha Omega) was penetrated perpendicularly into the contralesional or ipsilesional MI to identify the digit region. Parameters of electrical stimulation were as follows: trains of 11 and 44 cathodal pulses, 200-μs duration at 333 Hz, current of less than 65 μA. Basically, movements of the digits on the MI stimulation are easily elicited by short trains in a normal control (Miyachi et al. 2005). However, as we could assume that the movement threshold for ICMS might become higher after SCI, we used a 44-pulse train in addition to an 11-pulse train. Evoked movements of the digits were carefully monitored by visual inspection and muscle palpation.

Muscimol Injections

To confirm whether compensatory pathways arising from the contralesional MI might be involved in recovery from impaired manual dexterity in our SCI model, the gamma-aminobutyric acid type A ($GABA_A$) receptor agonist, muscimol (1 μg/μL in physiological saline, Sigma-Aldrich), was injected into the electrophysiologically identified digit region of the contralesional or ipsilesional MI through a 10-μL Hamilton microsyringe following ICMS. At each of 4 loci, 3 μL of muscimol was infused incrementally (Fig. 6A). Saline was injected into the same sites using the same parameters as a control. After the muscimol or saline injections into the MI digit region, skilled forelimb movements were assessed via the reaching/grasping task (for horizontal slots). Data were expressed as the ratio of successfully collected pellets to the total per session.

Anterograde Tract-Tracing of CST Fibers

CST fibers below the lesioned site arising from the contralesional MI were anterogradely labeled with BDA (BDA; Invitrogen; 10 000 MW). The BDA injections into the contralesional MI were performed 7 weeks prior to sacrifice as previously described (Nakagawa et al. 2015). Briefly, under general anesthesia (see above), a 10% solution of BDA in PBS was extensively injected into multiple loci along the central sulcus where regions representing not only the forelimb but also the trunk and hindlimb were located, through a 5-μL Hamilton microsyringe (150 nl each penetration) (Fig. 1B).

Motoneuron Labeling Through the Median Nerve

To label spinal motoneurons through the median nerve on the SCI side, a 5% solution of WGA-HRP in physiological saline (Sigma-Aldrich) was applied to the cut end of the nerve 4 days prior to sacrifice. Under deep-anesthesia conditions (see above), the skin and intermuscular septum of the arm were dissected, and the median nerve was exposed. The nerve was fully transected approximately 3.5 cm distal to the elbow joint. A total of 10 μL WGA-HRP was put inside a special tube, the cut end of the nerve was immersed in the tracer solution for 10 min, and then, the muscles and skin were sutured. Following the surgery, the monkeys were given the analgesic and antibiotic.

Histochemical and Immunohistochemical Procedures

Following sedation with ketamine hydrochloride (10 mg/kg, i.m.) and xylazine hydrochloride (1 mg/kg, i.m.), the monkeys were

anesthetized deeply with sodium pentobarbital (50 mg/kg, i.v.) and perfused transcardially with 10% formalin. The fixed brain and spinal cord were removed, immersed in PBS containing 30% sucrose until they sank, and then cut serially into 40-μm thick transverse sections (for the spinal cord) or 50-μm thick frontal sections (for the brain) on a freezing microtome. Procedures for histochemical visualization of injected and transported BDA with DAB-nickel and for immunohistochemistry with the Vector NovaRed substrate kit (Vector laboratories) were done as described elsewhere (Nakagawa et al. 2015). For immunofluorescence histochemical procedures, floating sections were blocked with 2% normal goat or donkey serum and 3% bovine serum albumin in PBS containing 0.1% Triton X-100 for 60 min. The sections were then incubated with primary antibodies for 120 min at room temperature (RT), followed by 2 overnights at 4 °C. Primary antibodies used in the present study were as follows: mouse anti-RGMa (IBL), rabbit anti-Iba1 (Wako), goat anti-ChAT (Millipore), mouse anti-NeuN (Millipore), goat anti-WGA (Vector laboratories), rabbit anti-WGA (Sigma-Aldrich), guinea pig anti-VGluT1 (Millipore), and sheep anti-Chx10 (Abcam) antibodies. The anti-WGA antibody was preabsorbed with powder of the monkey's brain and spinal cord for prevention of cross-reaction with unknown endogenous molecules. The goat anti-WGA antibody was used for all analyses except double immunostaining with the rabbit anti-WGA antibody in combination with the goat anti-ChAT antibody. BDA immunofluorescence histochemistry was carried out with Alexa Fluor 488-conjugated streptavidin 2 overnights at 4 °C. Subsequently, the sections were incubated with secondary antibodies for 120 min at RT in the dark. Secondary antibodies used in this study were as follows: goat and donkey anti-mouse, rabbit, goat, guinea pig, and sheep IgG Alexa Fluor 647, 568, and 488 (Invitrogen). To reduce endogenous autofluorescence, the sections were immersed in a TrueBlack (Biotium) solution diluted by 70% ethanol for 30 s. All histochemical and immunohistochemical images were acquired with a microscope (Biorevo BZ-9000, Keyence) or a confocal laser-scanning microscope (Fluo View FV1000, Olympus and LSM 800, Zeiss).

In Situ Hybridization Procedures

Under deep anesthesia (see above), the monkeys underwent perfusion-fixation with 4% paraformaldehyde (PFA) dissolved in 0.1 M phosphate buffer (PB; pH 7.4). The brain was removed and immersed in a 30% sucrose solution containing 4% PFA at 4 °C overnight. In situ hybridization was performed as previously described with minor modifications (Watakabe et al. 2007). Briefly, 40-μm thick frontal sections were placed onto glass slides (Thermo Fisher Scientific) and fixed with 4% PFA in PB for 15 min at RT. The sections were treated sequentially with proteinase K (7.2 μg/mL) for 30 min at 37 °C, 4% PFA for 15 min at RT, 0.25% acetic anhydride in 0.1 M triethanolamine for 10 min at RT, 0.3% Triton X-100 in PB for 20 min at RT. Subsequently, the sections were hybridized with a Digoxigenin (DIG)-labeled riboprobe (0.12 μg/mL) for 16 h at 68 °C in a hybridization buffer comprising 50% formamide, 5× SSC, 5× Denhard's solution (Invitrogen), 250 μg/mL tRNA (Roche Diagnostics), 500 μg/mL ssDNA (Sigma-Aldrich). The riboprobe for *Neogenin* (XM_015 142 632.1; 346–979) was purchased from Geno Staff (Tokyo, Japan) and heated at 80 °C for 5 min before use. After overnight, the sections were washed with 0.2× SSC for 30 min × 3 at 68 °C. Next, the sections were blocked with 1% blocking reagent (Roche Diagnostics) and 10% lamb serum in Tris-buffered saline containing 0.05% Tween 20 (TBS) for 1 h at RT and then incubated with alkaline phosphatase-conjugated anti-DIG antibody (1:5 000 dilution, Roche Diagnostics) in TBS containing 1% blocking reagent and 1% lamb serum for 2 h at RT. To visualize hybridization signals, the sections were immersed in a coloring buffer containing nitroblue tetrazolium and 5-bromo-4-chloro-3-indolyl phosphate.

Data Analyses

Quantification of BDA-Labeled CST Fibers Below the Lesioned Site

BDA-labeled CST fibers in the C7, C8, and Th1 segments were quantified in laminae VII and IX of transverse sections (400 μm apart) on the SCI side. Additionally, BDA-labeled midline-crossing fibers from the ipsilateral and ventral CSTs were quantified in each segment below the lesioned site. In lamina VII, the intensity of BDA-labeled CST fibers stained by DAB reaction was measured within a rectangular area (273 μm high × 362 μm wide) that was located 800 μm lateral to the center of the central canal using an ImageJ software (National Institutes of Health, Bethesda, MD, USA). Regarding lamina VII or IX, the number of contacts of BDA-labeled CST fibers with single Chx10-labeled neuron (Immunofluorescence) or single WGA-HRP-labeled motoneurons (DAB staining) was analyzed at a magnification of ×400, respectively. The contacts were defined by the presence of button-like swellings of BDA-labeled CST fibers on somas or dendrites. The result was normalized by the mean number of BDA-labeled CST fibers in the dorsolateral area at the C5 segment (3 serial sections) on the SCI side. BDA-labeled CST fibers that were observed in the gray matter within a radius of 50 μm from the midline of the spinal cord on each of the SCI and non-SCI sides were counted as midline-crossing fibers from the ipsilateral and ventral CSTs (Fig. 5*U*). It should be noted here that such midline-crossing fibers may contain some contralaterally sprouting CST fibers. The result was normalized by the mean number of BDA-labeled CST fibers in the dorsolateral area at each segment (3 serial sections) on the non-SCI side.

Measurements of the Extent of Spinal Cord Lesions

The extent of spinal cord lesions was measured, with the ImageJ software described above, as the mean maximum lesioned area in 3 serial sections Nissl-stained with 1% Cresyl violet (Nakagawa et al. 2015). The lesioned area was expressed as the ratio to the total area of the hemi-transverse section on the lesioned side.

Statistics

For behavioral analyses of the control antibody-treated and anti-RGMa antibody-treated monkey groups, a 2-way ANOVA was applied. Increases in BDA-labeled CST fibers in laminae VII, IX, and the midline area (i.e., midline-crossing CST fibers) were also analyzed by 2-way ANOVA, followed by a Student's *t*-test. For within-group comparisons for premuscimol versus postmuscimol injections in the reaching/grasping task, and for the extent of spinal lesions, paired *t*-tests were applied. All data were represented as mean ± standard error of the mean (SEM), and statistical significance was accepted at $P < 0.05$.

Results

SCI Model and the Extent of Spinal Cord Lesions

In our SCI model, the spinal cord was unilaterally lesioned in macaque monkeys. The lesions were made at the border between the C6 and the C7 level to infringe upon the lateral

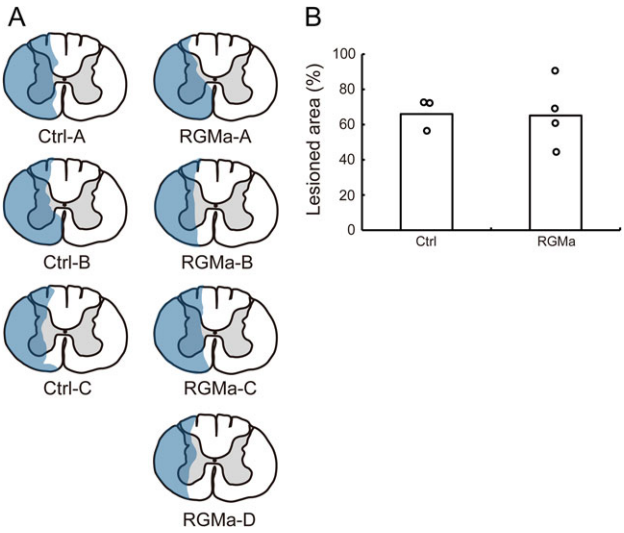

Figure 2. Extent of spinal cord lesions. (*A*) Extent of SCI (in blue) in a representative transverse section in each monkey. (*B*) Ratio of the lesioned area to the total area in a hemisection in each of the control antibody-treated (Ctrl) and anti-RGMa antibody-treated (RGMa) monkeys. There is no marked difference in the averaged ratio between the 2 monkey groups. Because of death from an unknown cause shortly after the behavioral analyses, monkey RGMa-B was excluded from the electrophysiological/pharmacological and histological analyses.

area of the hemitransverse section (Fig. 1*A*). When BDA was injected into the contralateral (contralesional) MI, laterally situated CST fibers were found to be fully removed in all of the lesioned monkeys, and no BDA-labeled CST fibers were observed in the dorsolateral funiculus of the spinal cord below the lesioned site (Figs 1*B*-*E*,*G*–*I* and 2*A*; see also Fig. 5*B*,*G*,*L*). The lesioned sites in all SCI monkeys were Nissl-stained to assess the ratio of the lesioned area, and there was no marked difference between the control antibody-treated (control) monkey group and the anti-RGMa antibody-treated (RGMa antibody-treated) monkey group (Fig. 2*A*,*B*). Part of the medial gray matter was kept intact to retain a route of sprouting CST fibers in our SCI model, and anterograde tract-tracing with BDA from the contralesional MI resulted in CST fiber labeling in this area (Figs 1*C*,*D*,*F*,*H*,*J* and 2*A*). To confirm cross-reaction of the anti-RGMa antibody to the MI and the spinal cord of rhesus monkeys, western blotting was performed. We observed double and triple bands in the monkey MI and spinal cord (Fig. 1*M*). It has been reported that the RGMa protein is a tethered membrane-bound molecule, and that proteolytic processing amplifies RGMa diversity by creating soluble versions, the full-length and proteolytic cleavage RGMa, with long-range effects (Tassew et al. 2009, 2012). The antibody was delivered continuously to the lesioned site via the osmotic pump for 4 weeks immediately after SCI (Fig. 1*K*,*L*,*N*).

Upregulation of RGMa Around the Lesioned Site After SCI

First, the expression patterns of RGMa and *Neogenin* (a receptor for RGMs) were examined by immunohistochemistry or in situ hybridization in the cervical cord or MI, respectively, in our SCI model (one intact and 2 lesioned monkeys; Fig. 3). Longitudinal sections in the cervical cord 10 days after SCI were immunostained with the anti-RGMa antibody, and then RGMa expression was compared with a region remote from the lesioned site in the same section and with the same region in an intact (uninjured) section (Fig. 3*A*–*C*,*F*). Our immnunohistochemical analyses revealed that RGMa expression increased significantly around the lesioned site after SCI. Next, we characterized RGMa-expressing cells by double immunofluorescence histochemistry and found that RGMa was present in Iba1-positive cells (Fig. 3*D*–*F*). Thus, RGMa was expressed in microglia/macrophages and upregulated specifically around the lesioned site. In addition, *Neogenin* was expressed in Layer 5 (identified in the adjacent Nissl-stained sections) of the contralesional and ipsilesional MI (Fig. 3*G*–*J*).

Effects of Anti-RGMa Antibody on Impaired Manual Dexterity After SCI

In the reaching/grasping task, the motor performance through both the vertical-slot and the horizontal-slot tasks was greatly recovered in the RGMa antibody-treated monkey group, compared with the control monkey group, to reach as highly as the pre-SCI level (Fig. 4*C*,*D*, Video S1). Similar results were obtained in the modified Brinkman board test, especially when the RGMa antibody-treated monkey group took out pellets from vertical slots (Fig. 4*F*,*G*, Video S2). In the case where skilled forelimb movements in the horizontal-slot task were attempted, the RGMa antibody-treated monkey group did not exhibit prominent functional recovery, although motor behavior improved relative to the control monkey group in which no such movements were restored (Fig. 4*H*, Video S2). Moreover, our behavioral analyses revealed that in both the reaching/grasping task and the modified Brinkman board test, the antibody treatment against RGMa not only promoted the recovery of motor functions but also advanced the start of recovery following SCI (Fig. 4*C*,*D*,*F*–*H*).

Increase in Sprouting CST Fibers With a Neutralizing Antibody Against RGMa

To begin with addressing the reorganization of CST fibers below the lesioned site, we analyzed the distribution pattern of BDA-labeled CST fibers in the C7, C8, and Th1 segments. We observed no BDA-labeled CST fibers in the dorsolateral funiculus in either the control or the RGMa antibody-treated monkey groups (Fig. 5*A*,*B*,*F*,*G*,*K*,*L*). Approximately 30–50% of the BDA-labeled CST fibers, relative to an intact monkey, were found in lamina VII of the RGMa antibody-treated monkey group, whereas less than 10% were seen in lamina VII of the control monkey group (Fig. 5*A*,*C*,*F*,*H*,*K*,*M*,*P*). In lamina IX, all WGA-HRP-labeled neurons corresponded with ChAT-positive motoneurons (Fig. 5*D*′), indicating that all are motoneurons for the median nerve. In the RGMa antibody-treated monkey group, the number of contacts of sprouting CST fibers with single WGA-positive neurons increased in lamina IX below the lesioned site compared with the control monkey group (Fig. 5*A*, *D*,*E*,*F*,*I*,*J*,*K*,*N*,*O*,*Q*,*E*′). At least part of the sprouting CST fibers seemed to be in contact with spinal interneurons immunolabeled for Chx10. Similarly, we observed that the sprouting CST fibers in the RGMa antibody-treated monkey group appeared to make contact with single Chx10-positive neurons more frequently than in the control monkey group (Fig. 5*W*–*C*′). We found a certain difference in the reinnervation pattern of sprouting CST fibers in each segment. In lamina VII, the intensity of BDA-labeled CST fibers and the number of contacts of these CST fibers with single Chx10-positive neurons gradually decreased in the RGMa antibody-treated monkey group as the

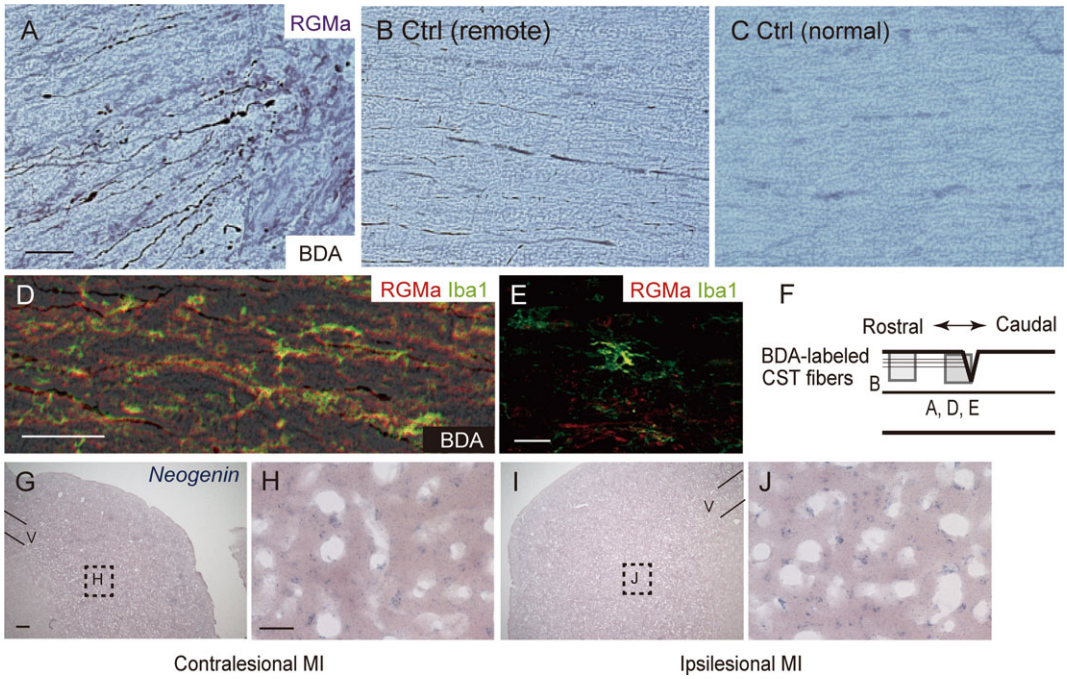

Figure 3. Expression patterns of RGMa and *Neogenin* in the cervical cord and MI. (*A*) RGMa expression (in purple) around the lesioned site (at the C6/C7 border) 10 days after SCI in a longitudinal section. Shown in black are CST fibers anterogradely labeled after BDA injections into the contralesional MI. (*B*) RGMa expression in a region remote from the lesioned site in the same section. (*C*) RGMa expression in the same region as in panel A in a normal (uninjured) case. (*D* and *E*) Expression of RGMa in combination with Iba1 around the lesioned site. (*F*) Schematic diagram representing the approximate locations of panels *A*, *B*, *D*, and *E*. (*G*) In situ hybridization for *Neogenin* messenger RNA in layer 5 (V) of the contralesional MI 10 days after SCI in a frontal section. (*H*) Higher power magnification of the boxed area in panel *G*. (*I*) In situ hybridization for *Neogenin* messenger RNA in layer 5 (V) of the ipsilesional MI 10 days after SCI in a frontal section. (*J*) Higher power magnification of the boxed area in panel I. Scale bars, *A*: 50 μm for A–C; *D*, *G*, *I*: 200 μm; *E*, *H*, *J*: 50 μm.

distance from the lesioned site became larger (C7 < C8 < Th1). By contrast, the number of contacts of sprouting CST fibers with single WGA-positive neurons increased in this group, similar to the findings in an intact monkey (Fig. 5P,Q,C′). The number of midline-crossing fibers also increased with the neutralizing antibody against RGMa (Fig. 5R–V). It should be noted here that the midline-crossing fibers observed may involve some extended fibers from the injured CST.

Impairments in Recovered Manual Dexterity by Muscimol Inactivation in the Contralesional MI

Following all behavioral analyses, ICMS was performed in the contralesional and ipsilesional MI of both the control and the RGMa antibody-treated monkey groups to determine whether the contralesional MI might contribute to functional recovery from impaired manual dexterity due to SCI (Fig. 1N). Movements of the digits ipsilateral to the SCI were successfully elicited by ICMS in 4 loci of the contralesional MI, but not of the ipsilesional MI in the RGMa antibody-treated SCI monkeys (Fig. 6A). Subsequent injections of muscimol into all of the electrophysiologically identified digit regions of the contralesional MI, but not of the ipsilesional MI, induced reversible impairments in skilled forelimb movements on the SCI side (Fig. 6C,D). The reaching/grasping task (for horizontal slots) was employed to assess motor function, and after approximately 20 min following muscimol injections, manual dexterity gradually deteriorated and became severely impaired within 1 h. Thereafter, impaired forelimb movements were continually seen for a duration of a few hours. Although all RGMa antibody-treated monkeys could move the digits individually the following day, manual dexterity was not sufficiently restored, as compared with that before the muscimol injections into the contralesional MI. When we carried out the ICMS experiment in the control monkey group, no movements of the digits were evoked in the contralesional MI (Fig. 6B). In general, the digit region of the MI was surrounded by the regions representing the wrist, elbow, and face in macaque monkeys (Sessle and Wiesendanger 1982). However, a sector surrounded by the wrist, elbow, and face regions exhibited no response to ICMS (Fig. 6B). As we could not identify the digit region in the contralesional MI of the control monkey group, we injected muscimol only into the ipsilesional MI. Then, the muscimol injections into the digit region of the ipsilesional MI induced reversible impairments in skilled movements of the SCI-unimpaired forelimb only on the uninjured side (Fig. 6E), just like the RGMa antibody-treated monkey group (Fig. 6D).

Discussion

Owing to the low capacity of growth/regeneration in the mature CNS, various therapeutic approaches to CNS injuries have been investigated against extrinsic and intrinsic inhibiting factors using in vivo and in vitro experiments with rodents (Sandvig et al. 2004; Hata et al. 2006; Mar et al. 2014). According to previous research (Yiu and He 2006; Popovich and Longbrake 2008; Rolls et al. 2009), glial cells expressing growth-inhibiting factors are rich in the lesioned area after SCI in rodents, and immune and inflammatory cells also accumulate in this area. It has been repeatedly demonstrated that RGMa is expressed in these cells (Schwab et al. 2005; Mirakaj et al. 2010; Muramatsu et al. 2011). The present study revealed that RGMa was

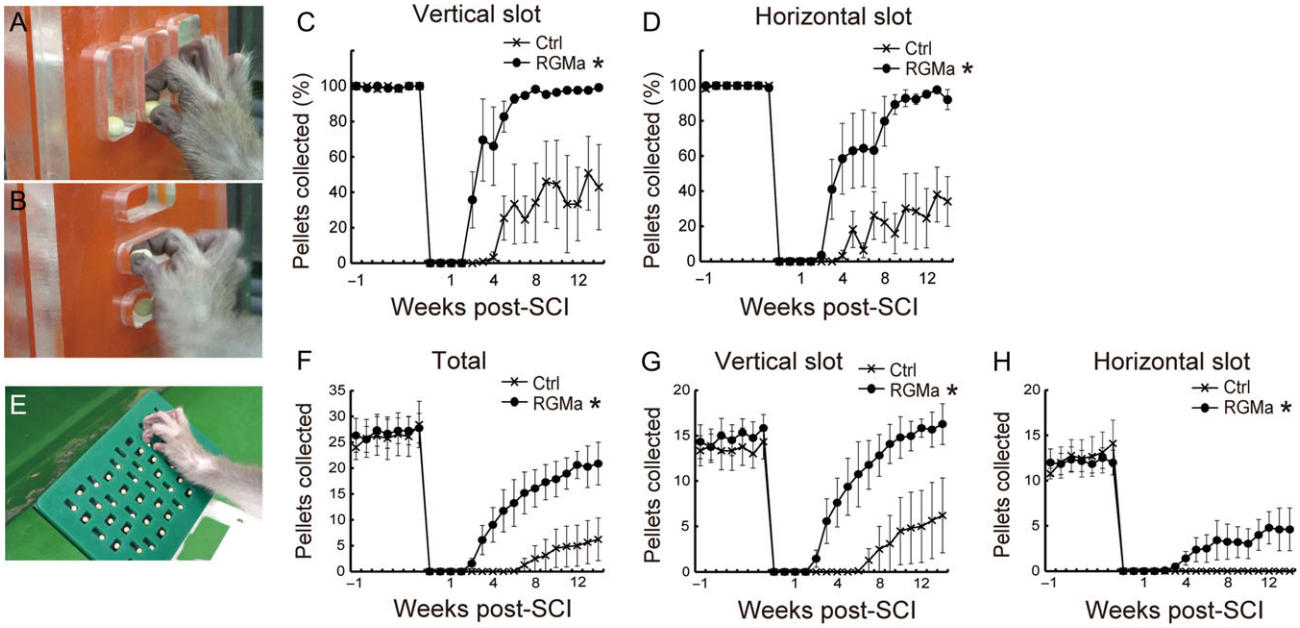

Figure 4. Recovery from impaired manual dexterity with the neutralizing antibody against RGMa. (*A* and *B*) Reaching/grasping task. The monkey reaches for vertical (*A*) or horizontal (*B*) slots and grasps pellets. (*C* and *D*) Ratio of pellets collected through vertical (*C*) or horizontal (*D*) slots. (*E*) Modified Brinkman board test. The monkey takes out pellets from randomly set vertical and horizontal slots. (*F*) Total number of pellets collected through vertical and horizontal slots. (*G* and *H*) Number of pellets collected through vertical (*G*) or horizontal (*H*) slots. All data are based on 3 control antibody-treated (Ctrl) and 4 anti-RGMa antibody-treated (RGMa) monkeys. Error bars denote SEM (2-way ANOVA, $^*P < 0.05$).

upregulated specifically around the lesioned site with increases in microglia/macrophages after SCI (Fig. 3*D*,*E*).

The spinal cord repair strategies involving growing/regenerating axons include a series of events, consisting of the initiation of axonal growth, the maintenance of axonal elongation, the connectivity with appropriate target neurons, and the reorganization of neural circuitry (Bradbury and McMahon 2006). In rodent SCI models, reaching/grasping behavior is promoted by enhanced sprouting CST fibers, and many of these fibers extend through the medial part of the spinal cord (Hollis et al. 2016). Thus, the enhanced sprouting of CST fibers would make a synaptic connection with spinal interneurons as the target for restoration of forelimb functions in rodents. For a precision grip in higher primates, corticomotoneuronal pathway neurons in the MI are specifically activated (Muir and Lemon 1983). Moreover, during the monkey's performance in a pinching task, motor commands descending to spinal motoneurons are mediated at least partly by the spinal interneurons (Takei and Seki 2010, 2013). Taken together, it is most likely that the reorganization of both the direct and the indirect (via the spinal interneurons) corticomotoneuronal pathways are required to promote recovery from impaired manual dexterity through enhanced sprouting of CST fibers in our SCI model.

In our behavioral tasks, to take out pellets skillfully from vertical and horizontal slots, cortically derived compensatory input should be transmitted to the motoneurons and/or interneurons in the C7, C8, and Th1 segments that are situated below the SCI site. Particularly when taking out a pellet from the horizontal slot in the modified Brinkman board test, the monkey is required to move the wrist in the ulnar direction to achieve digit flexion with ulnar deviation. It has been reported that the wrist angle in the ulnar direction is largely reduced after SCI when monkeys take out pellets from the horizontal slot (Hoogewoud et al. 2013). In macaque monkeys, spinal motoneurons innervating the extensor carpi ulnaris muscle responsible for digit flexion with ulnar deviation are mainly distributed in the C8 and Th1 segments (Jenny and Inukai 1983; Schieber 1995).

We demonstrated that sprouting CST fibers originating from the contralesional MI in RGMa antibody-treated monkeys penetrated more densely relative to the control monkey group into laminae VII and IX below the lesioned site, where spinal interneurons and motoneurons are located, respectively (Fig. 5*P*,*Q*). In our experiments, the motoneurons in the C7, C8, and Th1 segments were labeled through the median nerve that predominantly governs the distal forelimb muscles, activity of which is essential for execution of manual dexterity with a precision grip (Dun et al. 2007). In addition, a large number of motoneurons for hand (digits) muscles in primates are located in the Th1 segment (Jenny and Inukai 1983). With respect to the pattern of reinnervation of the enhanced corticomotoneuronal pathway after SCI with the anti-RGMa antibody treatment, sprouting CST fibers might lead to appropriate target motoneurons with guidance factors to promote effective and efficient recovery of motor functions.

At least part of the sprouting CST fibers seemed to be in contact with the interneurons immunolabeled for Chx10. Chx10 was originally identified as one of the markers for glutamatergic interneurons in rodents (Ericson et al. 1997), and Chx10-positive neurons are reportedly distributed throughout the hindbrain and the spinal cord in mammals and regulate motor functions, such as breathing and locomotion (AI-Mosawie et al. 2007; Crone et al. 2008, 2012; Dougherty and Kiehn 2010; Azim et al. 2014). According to recent work (Liu et al. 2015), there is a correlation between the number of Chx10-positive neurons in contact with sprouting CST fibers and functional recovery of the forelimb with unilateral cervical cord injury in mice. Together with the direct corticomotoneuronal pathway, the compensatory indirect pathway via spinal interneurons may also be crucial to the recovery of a series of forelimb movements in our SCI model, including reaching for slots and taking out pellets from slots using precision grip.

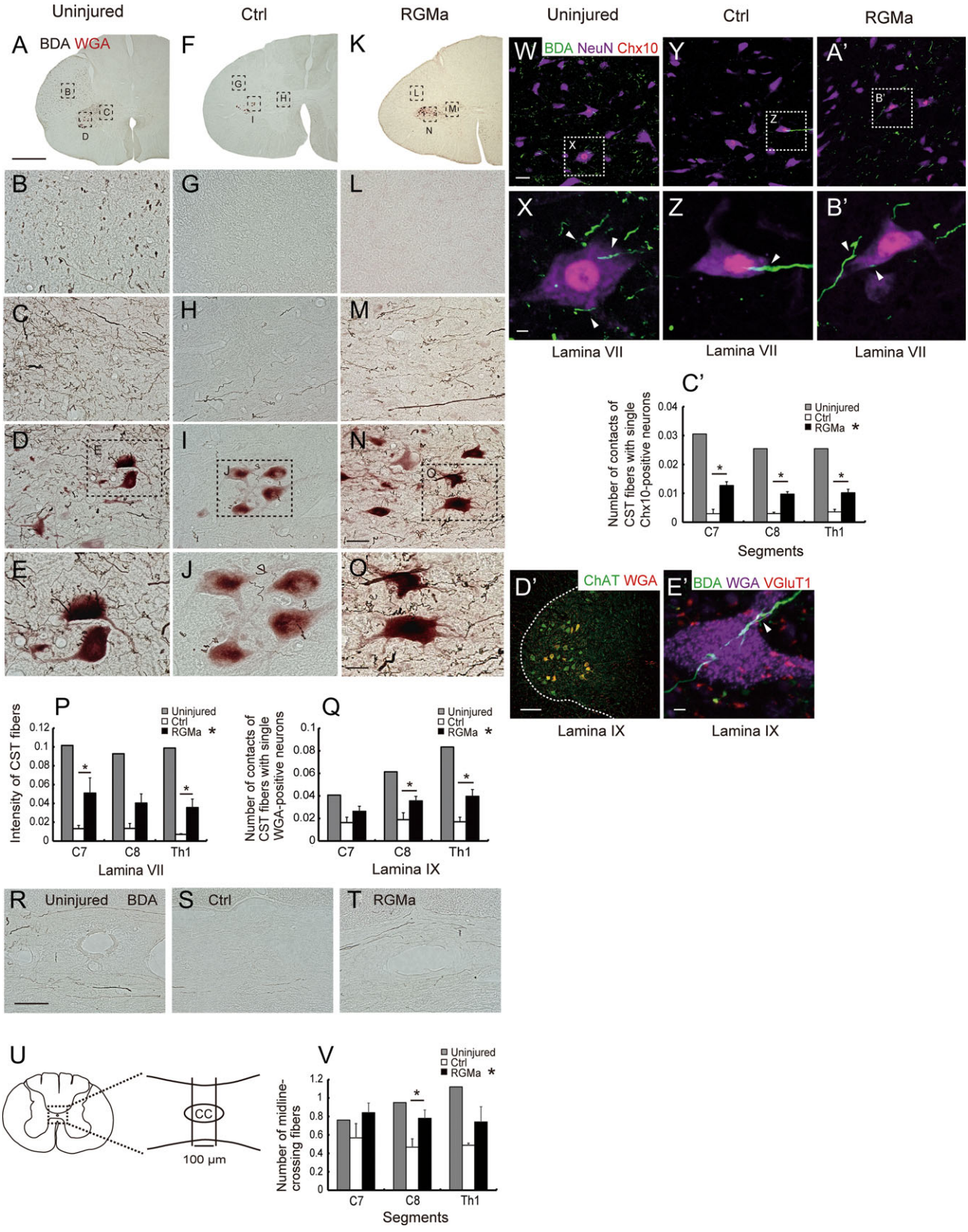

Figure 5. Sprouting of CST fibers with the neutralizing antibody against RGMa. (*A*, *F*, and *K*) BDA-labeled CST fibers in the Th1 segment in an intact (Uninjured; *A*), control antibody-treated (Ctrl; *F*), and anti-RGMa antibody-treated (RGMa; *K*) monkey. (*B*, *G*, and *L*) Higher power magnifications of areas of the dorsolateral funiculus in panels *A*, *F*, and *K*, respectively. (*C*, *H*, *M*, *D*, *I*, and *N*) Higher power magnifications of areas of laminae VII (*C*, *H*, and *M*) and IX (*D*, *I*, and *N*) in panels *A*, *F*, and *K*, respectively. (*E*, *J*, and *O*) Higher power magnifications of dotted zones in panels *D*, *I*, and *N*, respectively. (*P*) Intensity of BDA-labeled CST fibers in lamina VII in the intact (uninjured; $n = 1$), control antibody-treated (Ctrl; $n = 3$), and anti-RGMa antibody-treated (RGMa; $n = 3$) monkey groups. (*Q*) Number of contacts of BDA-labeled CST

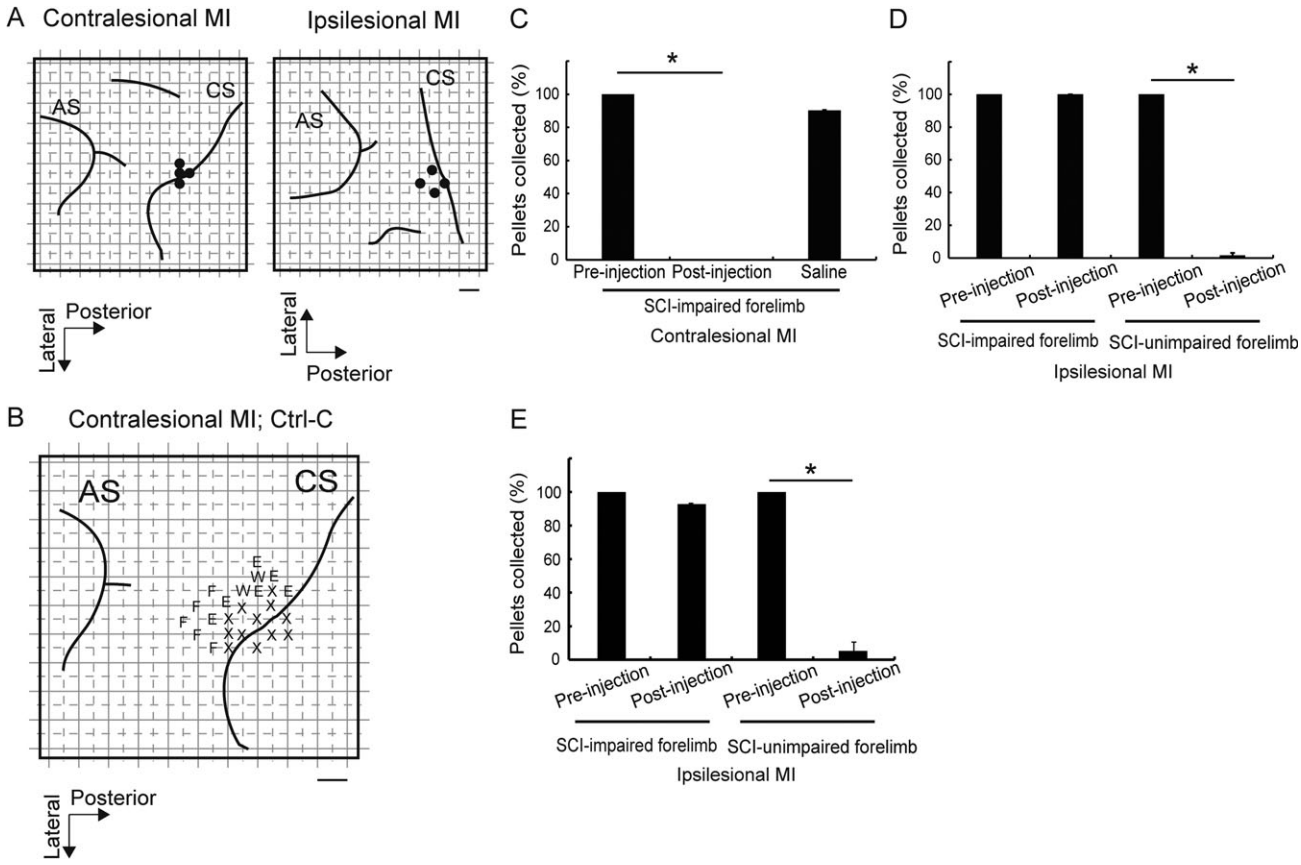

Figure 6. Effects of muscimol injections into the MI on manual dexterity. (*A*) Sites of muscimol injections into the contralesional and ipsilesional MI in a representative anti-RGMa antibody-treated monkey (RGMa-A). Filled circles indicate the injection loci in which ICMS induced movements of the digits on the contralateral side. AS, arcuate sulcus; CS, central sulcus. Scale bar, 2 mm. (*B*) Results of ICMS mapping of the contralesional MI in a representative control antibody-treated monkey (Ctrl-C). Each letter denotes the electrophysiologically identified body part as follows: E, elbow; F, face; W, wrist; X, no response. Scale bar, 2 mm. (*C*–*E*) Skilled movements after muscimol injections into the digit region of the contralesional MI (*C*) or the ipsilesional MI (*D*) in the anti-RGMa antibody-treated monkey group ($n = 3$), or of the contralesional MI in the control antibody-treated monkey group (*E*; $n = 3$). Manual dexterity that had been impaired by SCI and then recovered by RGMa treatment (SCI-impaired forelimb) was again impaired after muscimol (but not saline) injections into the contralesional MI. On the other hand, the muscimol injections into the ipsilesional MI only caused impairments in skilled movements of the normal forelimb (SCI-unimpaired forelimb) contralateral to the injections. Error bars indicate SEM (Student's *t*-test, $^*P < 0.05$).

Interestingly, according to our behavioral analyses, the antibody treatment against RGMa not only promoted the recovery of motor functions, that is, the ability to move the digits individually but also advanced the start of recovery following SCI. It has been well documented that treatment with the RGMa-neutralizing antibody in a rodent model of multiple sclerosis promotes functional recovery by preventing neurodegeneration (Muramatsu et al. 2011; Tanabe and Yamashita 2014; Demicheva et al. 2015). Recently, it was reported that an antibody treatment against RGMa promoted neuronal survival around lesioned sites with improvement of functional recovery in a rodent SCI model (Mothe et al. 2017). Moreover, RGMa has been shown to reduce leukocyte trafficking and retard inflammation (Mirakaj et al. 2010). Thus, RGMa suppression has a certain impact on neuroprotection as well as on neurite outgrowth, and the present results might therefore be ascribed, at least partly, to the neuroprotective effect of the RGMa antibody.

The spinal cord lesions in some cases (i.e., Ctrl-B and RGMa-A monkeys) infringed to some extent upon uncrossed ventral CST regions, though it generally did not affect recovery of manual dexterity, especially in the RGMa antibody-treated (RGMa-A) monkey (data not shown). It has previously been reported that the ventral CST distributes the fibers to proximal muscles, such as the neck, trunk, and proximal upper extremities (Nyberg-

fibers with single WGA-positive motoneurons in lamina IX in the same monkey groups as in panel *P*. (*R*, *S*, and *T*) BDA-labeled CST fibers crossing the midline of the spinal cord in an intact (Uninjured; *R*), control antibody-treated (Ctrl; *S*), and anti-RGMa antibody-treated (RGMa; *T*) monkey. BDA was injected into the contralateral or contralesional MI. (*U*) Schematic diagram showing the midline area examined. CC, central canal. (*V*) Number of midline-crossing CST fibers below the lesioned site (i.e., C7, C8, and Th1 segments). (*W*, *Y*, and *A′*) Spinal interneurons triple-labeled for BDA, NeuN, and Chx10 in lamina VII of the Th1 segment in an intact (Uninjured; *W*), control antibody-treated (Ctrl; *Y*), and anti-RGMa antibody-treated (RGMa; *A′*) monkey. (*X*, *Z*, and *B′*) Higher power magnifications of dotted zones in panels *W*, *Y*, and *A′*, respectively. BDA-labeled CST fibers in contact with single Chx10-positive neurons (specified by arrowheads). (*C′*) Number of contacts of BDA-labeled CST fibers with single Chx10-positive neurons in lamina VII in the same monkey groups as in panels *P* and *Q*. (*D′*) Motoneurons double-labeled for WGA-HRP through the median nerve and ChAT in lamina IX of the Th1 segment in an anti-RGMa antibody-treated monkey. All WGA-HRP-labeled neurons are ChAT-positive. The dotted line indicates the border between the gray and white matter. (*E′*) Triple labeling for BDA, WGA-HRP, and VGluT1 in lamina IX of the Th1 segment in an anti-RGMa antibody-treated monkey. A BDA-labeled CST fiber in contact with a single WGA-positive motoneuron (specified by arrowheads). Scale bars, *A*: 1 mm for *A*,*F*,*K*; *N*: 100 μm for *B*–*D*, *G*–*I*, *L*–*N*; *O*: 50 μm for *E*, *J*, and *O*; R: 100 μm for *R*, *S*, and *T*; *W*: 200 μm for *W*, *Y* , and *A′*; *X* and *D′*: 5 μm for *X*, *Z*, *B′*, and *D′*; *C′*: 200 μm. Error bars denote SEM (2-way ANOVA, followed by Student's *t*-test, $^*P < 0.05$).

Hansen 1963; Davidoff 1990; Canedo 1997). The motor tasks that we used in the present work (i.e., reaching/grasping task and the modified Brinkman board test) are required for movements of the proximal upper limb, but the spinal region responsible for the proximal upper limb remains intact in our SCI model.

By carrying out a series of pharmacological experiments following ICMS, we have demonstrated that the contralesional MI is significantly involved in recovery from impaired manual dexterity in our SCI model with anti-RGMa antibody treatment. In the control monkey group, on the other hand, forelimb movements once impaired by SCI could not be evoked using our ICMS protocol (44-pulse train, 65 μA current). This may depend on an increase in sprouting CST fibers from the contralesional MI to the cervical cord on the injured side. Additionally, it should be noted here that other descending pathways, including the corticobrainstem and corticopropriospinal pathways, might contribute to functional recovery (Isa et al. 2013). In a similar primate model of SCI (C7/C8 lesion model), reorganization of CST fibers originating from the contralesional MI with the somatotopic map altered is crucial to recovery of motor functions (Schmidlin et al. 2004, 2005). Parts of the uncrossed CST fibers derived from the ipsilesional MI were disrupted in our SCI model, and *Neogenin* was also expressed in layer 5 of the ipsilesional MI as well as of the contralesional MI (Fig. 3*I*,*J*). RGMa was demonstrated to evoke the strong inhibition of axonal outgrowth and regrowth through the transmembrane receptor Neogenin (Tassew et al. 2014). Hence, it can be considered that injured CST fibers extend beyond the lesioned site through the ipsilesional MI by the aid of the anti-RGMa antibody. However, the CST fibers through the ipsilesional MI may not work as functional wiring at a late stage after SCI. In view of the fact that the ipsilesional MI is activated at an early but not a late stage of recovery in a different primate model of SCI (Nishimura et al. 2007), the ipsilesional MI might participate in functional restoration only transiently.

The present study concludes that RGMa is a critical target molecule to promote recovery from impaired manual dexterity after SCI. The antibody treatment against RGMa may additionally be applied not only to SCI, but also to other CNS injuries, such as traumatic brain injuries, stroke, and multiple sclerosis.

Supplementary Material

Supplementary data are available at *Cerebral Cortex* online.

Funding

Core Research for Evolutional Science and Technology (CREST) program from the Japan Science and Technology Agency; the Strategic Research Program for Brain Sciences from the Japan Agency for Medical Research and Development; and by Grants-in-Aid for Scientific Research in Innovative Areas (to M.T., 15H01434) and for Young Scientists (B) (to H.N.) from the Ministry of Education, Culture, Sports, Science, and Technology of Japan.

Notes

We thank K. Koide, R. Yasukochi, Y. Takata, and H. Yamanaka for technical assistance, and Dr. A. MacIntosh for language editing of the article. The authors declare no competing financial interests. *Conflict of Interest*: None declared.

References

AI-Mosawie A, Wilson JM, Brownstone RM. 2007. Heterogeneity of V2-derived interneurons in the adult mouse spinal cord. Eur J Neurosci. 26:3003–3015.

Azim E, Jiang J, Alstermark B, Jessell TM. 2014. Skilled reaching relies a V2a propriospinal internal copy circuit. Nature. 508: 357–363.

Bradbury EJ, McMahon SB. 2006. Spinal cord repair strategies: why do they work? Nat Rev Neurosci. 7:644–653.

Canedo A. 1997. Primary motor cortex influences on the descending and ascending systems. Prog Neurobiol. 51:287–335.

Crone SA, Quinlan KA, Zagoraiou L, Droho S, Restrepo CE, Lundfald L, Endo T, Setlak J, Jessell TM, Kiehn O, et al. 2008. Genetic ablation of V2a ipsilateral interneurons disrupts left-right locomotor coordination in mammalian spinal cord. Neuron. 60:70–83.

Crone SA, Viemari JC, Droho S, Mrejeru A, Ramirez JM, Sharma K. 2012. Irregular breathing in mice following geneticablation of V2a neurons. J Neurosci. 32:7895–7906.

Davidoff RA. 1990. The pyramidal tract. Neurology. 40:332–339.

Demicheva E, Cui YF, Bardwell P, Barghom S, Kron M, Meyer AH, Schmidt M, Gerlach B, Leddy M, Barlow E, et al. 2015. Targeting repulsive guidance molecule A to promote regeneration and neuroprotection in multiple sclerosis. Cell Rep. 10:1887–1898.

Dougherty KJ, Kiehn O. 2010. Functional organization of V2a-related locomotor circuits in the rodent spinal cord. Ann NY Acad Sci. 1198:85–93.

Dun S, Kaufmann RA, Li ZM. 2007. Lower median nerve block impairs precision grip. J Electromyogr Kinesiol. 17:348–354.

Ericson J, Rashbass P, Schedl A, Brenner-Morton S, Kawakami A, van Heyningen V, Jessell TM, Briscoe J. 1997. Pax6 controls progenitor cell identify and neuronal fate in response to graded Shh signaling. Cell. 90:1169–1180.

Freund P, Schmidlin E, Wannier T, Bloch J, Mir A, Schwab ME, Rouiller EN. 2006. Nogo-A–antibody treatment enhances sprouting and functional recovery after cervical lesion in adult primates. Nat Med. 12:790–792.

Freund P, Schmidlin E, Wannier T, Bloch J, Mir A, Schwab ME, Rouiller EN. 2009. Anti-Nogo–A antibody treatment promotes recovery of manual dexterity after unilateral cervical lesion in adult primates—re-examination and extension of behavioral data. Eur J Neurosci. 29:983–996.

GrandPré T, Li S, Strittmatter SM. 2002. Nogo-66 receptor antagonist peptide promotes axonal regeneration. Nature. 417:547–551.

Hata K, Fujitani M, Yasuda Y, Doya H, Saito T, Yamagishi S, Mueller BK, Yamashita T. 2006. RGMa inhibition promotes axonal growth and recovery after spinal cord injury. J Cell Biol. 173:47–58.

Hollis ER 2nd, Ishiko N, Yu T, Lu CC, Haimovich A, Tolentino K, Richman A, Tury A, Wang SH, Pessian M, et al. 2016. Ryk controls remapping of motor cortex during fanctional recovery after spinal cord injury. Nat Neurosci. 19:697–705.

Hoogewoud F, Hamadjida A, Wyss AF, Mir A, Schwab ME, Belhaj-Saif A, Rouiller EM. 2013. Comparison of functional recovery of manual dexterity after unilateral spinal cord lesion or motor cortex lesion in adult macaque monkeys. Front Neurol. 4:101.

Isa T, Kinoshita M, Nishimura Y. 2013. Role of direct vs. indirect pathways from the motor cortex to spinal motoneurons in the control of hand dexterity. Front Neurol. 4:191.

Jenny AB, Inukai J. 1983. Principles of motor organization of the monkey cervical spinal cord. J Neurosci. 3:567–575.

Lah GL, Key B. 2012. Dual roles of the chemorepellent axon guidance molecule RGMa in establishing pioneering axon tracts and neural fate decisions in embryonic vertebrate forebrain. Dev Neurobiol. 72:1458–1470.

Lemon RN. 1993. The G. L. Brown Prize Lecture. Cortical control of the primate hand. Exp Physiol. 78:263–301.

Liu ZH, Yip PK, Adams L, Davies M, Lee JW, Michael GJ, Priestley JV, Michael-Titus AT. 2015. A single bolus of docosahexaenoic acid promotes neuroplastic changes in the innervation of spinal cord interneurons and motor neurons and improves functional recovery after spinal cord injury. J Neurosci. 35:12733–12752.

Mar FM, Bonni A, Sousa MM. 2014. Cell intrinsic control of axon regeneration. EMBO Rep. 15:254–263.

Matsunaga E, Nakamura H, Chedotal A. 2006. Repulusive guidance molecule plays multipleroles in neuronal differentiation and axon guidance. J Neurosci. 26:6082–6088.

Matsunaga E, Tauszing-Delamasure S, Monnier PP, Mueller BK, Strittmatter SM, Mehlen PCHedotal A. 2004. RGM and its receptor neogenin regulate neuronal survival. Nat Cell Biol. 6:749–755.

Mirakaj V, Brown S, Laucher S, Steinl C, Klein G, Köhler D, Skutella T, Meisel C, Brommer B, Rosenberger P, et al. 2010. Repulsive guidance molecule-A (RGM-A) inhibits leukocyte migration and mitigates inflammation. Proc Natl Acad Sci USA. 108:6555–6560.

Miyachi S, Lu X, Inoue S, Iwasaki T, Koike S, Nambu A, Takada M. 2005. Organization of multisynaptic inputs from prefrontal cortex to primary motor cortex as revealed by retrograde transneuronal transport of rabies virus. J Neurosci. 25: 2547–2556.

Monnier PP, Sierra A, Macchi P, Deitinghoff L, Andersen JS, Mann M, Flad M, Homberger MR, Stahl B, Bonhoeffer F, et al. 2002. RGM is a repulsive guidance molecule for retinal axons. Nature. 419:392–395.

Mothe AJ, Tassew NG, Shabanzadeh AP, Penheiro R, Vigouroux RJ, Huang L, Grinnell C, Cui YF, Fung E, Monnier PP, et al. 2017. RGMa inhibition with human monoclonal antibodies promotes regeneration, plasticity and repair, and attenuates neuropathic pain after spinal cord injury. Sci Rep. 7:10529.

Muir RB, Lemon RN. 1983. Corticospinal neurons with a special role in precision grip. Brain Res. 261:312–316.

Muramatsu R, Kubo T, Mori M, Nakamura Y, Fujita Y, Akutsu T, Okuno T, Taniguchi J, Kumanogoh A, Yoshida M, et al. 2011. RGMa modulates T cell responses and is involved in autoimmune encephalomyelitis. Nat Med. 17:488–494.

Nakagawa H, Ninomiya T, Yamashita T, Takada M. 2015. Reorganization of corticospinal tract after spinal cord injury in adult macaques. Sci Rep. 5:11986.

Nishimura Y, Onoe H, Morichika Y, Perfiliev S, Tsukada H, Isa T. 2007. Time-dependent central compensatory mechanisms of finger dexterity after spinal cord injury. Science. 318: 1150–1155.

Nyberg-Hansen R. 1963. Some comments on the pyramidal tract, with special reference to its individual variations in man. Acta Neurol Scand. 39:1–30.

Oudega M, Perez MA. 2012. Corticospinal reorganization after spinal cord injury. J Physiol. 590:3647–3663.

Popovich PG, Longbrake EE. 2008. Can the immune system be harnessed to repair the CNS? Nat Rev Neurosci. 9:481–493.

Rolls A, Shechter R, Schwartz M. 2009. The bright side of the glial scar in CNS repair. Nat Rev Neurosci. 10:235–241.

Rouiller EM, Yu XH, Moret V, Tempini A, Wiesendanger M, Liang E. 1998. Dexterity in adult monkeys following early lesion of the motor cortical hand area: the role of cortex adjacent to the lesion. Eur J Neurosci. 10:729–740.

Sandvig A, Berry M, Butt A, Longan A. 2004. Myelin-, reactive glia-, and scar-derived CNS axon growth inhibitors: expression, receptor signaling, and correlation with axon regeneration. Glia. 46:225–251.

Schieber MH. 1995. Muscular production of individuated finger movements: the roles of extrinsic finger muscles. J Neurosci. 15:284–297.

Schmidlin E, Wannier T, Bioch J, Belhaj-Saif A, Wyss AF, Ruiller EM. 2005. Reduction of the hand representation in the ipsilateral primary motor cortex following unilateral section on the corticospinal tract at cervical level in monkeys. BMC Neurosci. 6:56.

Schmidlin E, Wannier T, Bioch J, Ruiller EM. 2004. Progressive plastic change in the hand representation of the primary motor cortex parallel incomplete recovery from a unilateral section of the corticospinal tract at cervical level in monkeys. Brain Res. 1017:172–183.

Schwab JM, Conrad S, Monnier PP, Julien S, Mueller BK, Schluesener HJ. 2005. Spinal cord injury-induced lesional expression of the repulsive guidance molecule (RGM). Eur J Neurosci. 21:1569–1576.

Sessle BJ, Wiesendanger M. 1982. Structural and functional definition of the motor cortex in the monkey (*Macaca fascicularis*). J Physiol. 323:245–265.

Stahl B, Muller B, von Boxberg Y, Cox EC, Bonhoeffer F. 1990. Biochemical characterization of a putative axonal guidance molecule of the chick visual system. Neuron. 5:735–743.

Takei T, Seki K. 2010. Spinal interneurons facilitate coactivation of hand muscles during a precision grip task in monkeys. J Neurosci. 30:17041–17050.

Takei T, Seki K. 2013. Spinal premotor interneurons mediate dynamic and static motor commands for precision grip in monkeys. J Neurosci. 33:8850–8860.

Tanabe S, Yamashita T. 2014. Repulusive guidance molecule-a is involved in Th17-cell-induced neurodegeneration in autoimmune encephalomyelitis. Cell Rep. 9:1459–1470.

Tassew NG, Charish J, Chestopalova L, Monnier PP. 2009. Sustained *in vivo* inhibition of protein domains using single-chain Fv recombinant antibodies and its application to dissect RGMa activity on axonal outgrowth. J Neurosci. 29:1126–1131.

Tassew NG, Charish J, Seidah NG, Monnier PP. 2012. SKI-1 and Furin generate multiple RGMa fragments that regulate axonal growth. Dev Cell. 22:391–402.

Tassew NG, Mothe AJ, Shabanzadeh AP, Banerjee P, Koeberle PD, Bremner R, Tator CH, Monnier PP. 2014. Modifying lipid rafts promotes regeneration and functional recovery. Cell Rep. 8:11146–11159.

Vavrek R, Girgis J, Tetzlaff W, Hiebert GW, Fouad K. 2006. BDNF promotes connections of corticospinal neurons onto spared descending interneurons in spinal cord injured rat. Brain. 129:1534–1545.

Wahl AS, Omlor W, Rubio JC, Chen JL, Zheng H, Schröter A, Gullo M, Weinmann O, Kobayashi K, Helmchen F, et al. 2014. Neuronal repair. Asynchronous therapy restores motor control by rewiring of the rat corticospinal tract after stroke. Science. 34:1250–1255.

Watakabe A, Ichinohe N, Ohsawa S, Hashikawa T, Komatsu Y, Rockland KS, Yamamori T. 2007. Comparative analysis of layer-specific genes in mammalian neocortex. Cereb Cortex. 17:1918–1933.

Yiu G, He Z. 2006. Glial inhibition of CNS axon regeneration. Nat Rev Neurosci. 7:617–627.